Neutron study of local-environment effects in ferromagnetic Ni-Rh alloys*

J. W. Cable
Solid State Division, Oak Ridge National Laboratory, Oak Ridge, Tennessee 37830
(Received 15 November 1976)

Neutron diffuse-scattering measurements were made on Ni-Rh alloys containing 2-, 5-, 10-, 15-, 25-, 30-, and 35-at.% Rh to determine the spatial distribution of the magnetic moments. We find that $\bar{\mu}_{Ni}$ increases slightly out to about 5-at.% Rh, then decreases slowly to about 15-at.% Rh and beyond that decreases rapidly toward zero at the critical concentration of 37-at.% Rh. The concentration dependence of $\bar{\mu}_{Rh}$ is approximately described by a P_{12} dependence and is consistent with moments of $2\mu_B$ for those Rh atoms surrounded by 12 Ni nearest neighbors with a small residual moment of about $0.1\mu_B$ for Rh atoms with other environments. The diffuse cross sections exhibit small-K peaks which become sharper and more pronounced with increasing Rh content. These peaks show the presence of magnetic-moment fluctuations about the average moments and, from a comparison of the $K = 0$ intercepts with $d\bar{\mu}/dc$, we find that these fluctuations are due to local-environment effects. Because the range of these fluctuations increases with increasing Rh, we conclude that magnetic environment is important in determining the moment distribution of these alloys. The data are fitted to a local-environment model that includes the unusually large chemical-environment effect at Rh sites and both chemical- and magnetic-environment effects at Ni sites. The resulting parameters are physically reasonable and approach the correct limits at the extremes of the ferromagnetic region. One of the more interesting results of this fitting is that the chemical effect at Ni sites is positive, i.e., a Rh atom causes an increase in the moment of nearest-neighbor Ni atoms.

I. INTRODUCTION

The ferromagnetic Ni-Rh alloys exhibit an anomalous magnetization versus concentration behavior.[1,2] With increasing Rh content, the spontaneous magnetization first increases by about $2\mu_B$/Rh, then passes through a maximum near 4-at.% Rh before decreasing to zero at the critical concentration of 37-at.% Rh. A neutron measurement[3] in the dilute Rh region shows that the initial increase in magnetization is due to a large Rh moment ($\sim 2\mu_B$). One aim of the present neutron experiment is to determine the spatial distribution of the magnetic moments in an attempt to determine if the rapid loss of moment at higher concentrations is associated with competing ferro- and antiferromagnetic interactions as in the Ni-Mn system or with some other local-environment effect which destroys this large Rh moment. Another aim of the experiment is to answer a question raised by the magnetization results[2] in the critical region which indicate the presence of magnetic clusters similar to those found[4,5] for Ni-Cu alloys. This suggests that magnetic-environment effects occur in Ni-Rh since such effects are required[6-8] to explain the neutron data[7-9] for the Ni-Cu alloys. In this paper we explore this possibility by extending a recently developed[8] magnetic-environment model for nonmagnetic impurities in Ni to the case of magnetic impurities in Ni and by fitting this model to the neutron data.

II. CROSS SECTIONS

Magnetic diffuse-scattering cross sections were measured by both the unpolarized-neutron, field-off minus field-on method and the polarized-neutron, spin-up minus spin-down method. Both methods are well established and have been discussed in detail in recent papers[8,10] so only the necessary equations are presented here. The unpolarized cross section is given by

$$\frac{\Delta\, d\sigma}{d\Omega_{\text{unpol.}}}(K) = 0.0484c(1-c)T(K)\ , \tag{1}$$

in which c is the fractional impurity content and $T(K)$ is the Fourier transform of a two-site, moment-moment correlation. The polarized cross section is

$$\frac{\Delta d\sigma}{d\Omega_{\text{pol.}}}(K) = 1.08c(1-c)(b_i - b_h)M(K)\ , \tag{2}$$

where b_i and b_h are the impurity and host nuclear-scattering amplitudes and $M(K)$ is the Fourier transform of a site-occupation–moment correlation.

These $T(K)$ and $M(K)$ functions describe the moment disturbances caused by local environment in binary alloys. The $T(K)$ correlation has been treated by Marshall[11] for the case of linear response, and by Balcar and Marshall[12] for nonlinear response. The much simpler $M(K)$ correlation is readily obtained by use of their formalism and,

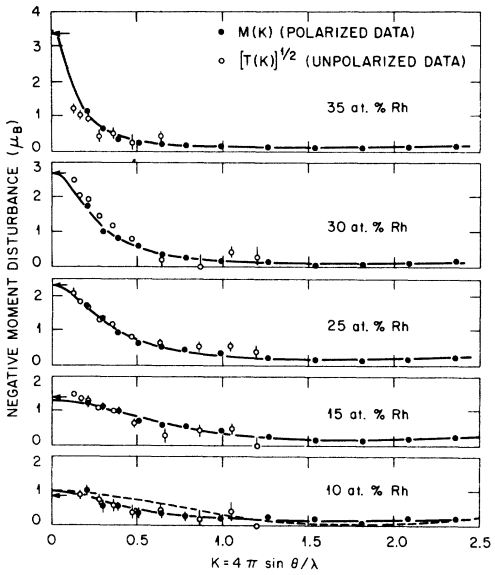

FIG. 1. K-dependent magnetic moment disturbances for concentrated Ni-Rh alloys. The solid curves are fitted to Eq. (8) while the dashed curve for 10-at.% Rh is a calculation based on the magnetic-environment model using interpolated parameters as described in the text. The arrows at $K=0$ represent the magnetization values of $d\bar{\mu}/dc$.

for these truly random Ni-Rh alloys, has the form

$$M(K)=\bar{\mu}_{\mathrm{Rh}} f_{\mathrm{Rh}}-\bar{\mu}_{\mathrm{Ni}} f_{\mathrm{Ni}}+(1-c)G(K)f_{\mathrm{Ni}}+cH(K)f_{\mathrm{Rh}}\ . \tag{3}$$

Here, $\bar{\mu}_{\mathrm{Rh}}$ and $\bar{\mu}_{\mathrm{Ni}}$ are the average Rh and Ni moments with form factors f_{Rh} and f_{Ni} while $G(K)$ and $H(K)$ are Fourier transforms of the Rh-induced moment disturbance at Ni sites and at Rh sites, respectively. This expression is valid for both linear and nonlinear response. In this local-environment model, the $K=0$ limits of these moment disturbance functions correspond to the concentration derivatives of the respective moments. Thus

$$M(0)=\frac{d\bar{\mu}}{dc}\ , \tag{4}$$

$$G(0)=\frac{d\bar{\mu}_{\mathrm{Ni}}}{dc}\ , \tag{5}$$

and

$$H(0)=\frac{d\bar{\mu}_{\mathrm{Rh}}}{dc}\ . \tag{6}$$

For polycrystalline samples, which require a spherically averaged $M(K)$, the $G(K)$ and $H(K)$ functions vanish at large K and $M(K)$ then yields the moment times form factor difference.

The corresponding $T(K)$ function is[12]

$$T(K)=[M(K)]^2+\cdots\ , \tag{7}$$

where the dots represent nonlinear terms. Thus, measurement of both $M(K)$ and $T(K)$ provides a determination of the nonlinear magnetic response of the alloy.

III. EXPERIMENTAL RESULTS

Ni-Rh alloys containing 2-, 5-, 10-, 15-, 25-, 30-, and 35-at.% Rh were prepared by arc melting and drop casting. Since negligible weight loss was observed, the nominal concentrations are assumed correct. X-ray analyses of the alloys showed a single fcc phase with lattice parameters in agreement with those reported by Luo and Duwez.[13] Neutron samples were cut from the cast ingots as flat polycrystalline plates with dimensions of approximately $2\times2.5\times0.2$ cm^3. These were annealed at 1000 °C for 24 h and then quenched.

Unpolarized-neutron cross sections were measured for all of the alloys as well as for a control sample of pure Ni which had been prepared in the same way. These measurements were made with 4.43-Å neutrons and a one-dimensional position-sensitive detector at the ORR. The sample temperature was maintained at 10 K and a 10-kOe field applied parallel to the plate was used to extract the magnetic part of the scattering. Absolute cross sections were obtained by calibration with a standard V scatterer. These range from about 1 mb for the 2- and 5-at.% Rh alloys to about 40 mb at small K for the more concentrated alloys. The expected null result was obtained to ±0.2 mb for the pure Ni sample. The field-on cross sections, which contain only the incoherent and the nuclear disorder scattering, show no K-dependent structure even for the more concentrated alloys thus reinforcing the previous conclusion[13] from x-ray data that these are random alloys. The observed $[T(K)]^{1/2}$ data are shown as the open circles in Figs. 1 and 2.

The polarized-neutron measurements were made at the HFIR (High Flux Isotope Reactor) using 1.07-Å neutrons. The samples were in symmetrical transmission geometry and were held at 4.2 K in a vertical magnetizing field of 20 kOe. The diffuse intensity inside of the first Bragg reflection was measured and corrected for instrumental background, incident polarization and flipper efficiency. No sample depolarization was detected. The magnetic cross sections were obtained by calibration against V and were corrected for slit height and for multiple Bragg scattering using the observed spin-dependent transmissions. Of these corrections, the multiple Bragg scattering is the most significant as well as the most difficult to calculate. However, by comparison of the observed and calculated spin-up *plus* spin-down cross sections, which contain multiple Bragg, incoherent, and nu-

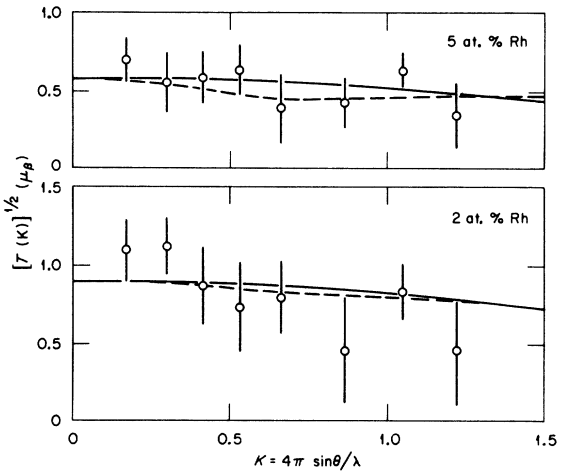

FIG. 2. K-dependent moment disturbances for dilute Ni-Rh alloys. The solid curves represent Eq. (3) with $\phi(K)=0$ while the dashed curves are calculated for the magnetic-environment model with interpolated parameters.

clear disorder scattering, we conclude that our multiple Bragg corrections are valid to ±15%. This correction increases with decreasing Rh content and below 10-at.% Rh the uncertainty in the multiple Bragg correction becomes comparable with the expected signal. The polarized neutron measurements were therefore confined to the 10–35-at.% Rh range. The results were converted to $M(K)$ values by use of Eq. (2) with nuclear amplitudes $b_{Rh}=0.584$ and $b_{Ni}=1.03\times10^{-12}$ cm. The $M(K)$ data are shown as the solid points in Fig. 1.

This figure illustrates some of the advantages of the polarized-neutron method. First, the sign of $M(K)$ is determined and this is negative for all of the alloys in Fig. 1. Also, the $M(K)$ data extend to larger-K values, where the spherically averaged $G(K)$ and $H(K)$ functions become negligible, and thus provide a better determination of the difference in average moments. The two principal advantages of the unpolarized method result from the use of long wavelength neutrons. These are: (i) there is no multiple Bragg scattering and (ii) the data extend to smaller K values and, in principle, should provide a better determination of the $K=0$ limit of the disturbance. For these particular data sets, there is more scatter in the $[T(K)^{1/2}$ data but there is general agreement between the $[T(K)]^{1/2}$ and $M(K)$ data. This indicates that nonlinear magnetic response is unimportant, at least for the cross sections, in these alloys. This is somewhat surprising in view of the distinctly nonlinear behavior of the bulk magnetization. However, we will find that the most pronounced nonlinearities occur at low Rh content where a comparison between $M(K)$ and $[T(K)]^{1/2}$ is lacking. Even so, the nonlinear terms enter Eq. (7) with a c dependence so it is probably valid to consider $[T(K)]^{1/2}\simeq M(K)$ for the dilute alloy results depicted in Fig. 2.

In fitting the $M(K)$ data to Eq. (3) we use $f_{Ni}=\exp(-0.044K^2)$ and $f_{Rh}=\exp(-0.099K^2)$ which closely approximate the experimental Ni and Pd form factors over this limited K region. Since $G(K)$ and $H(K)$ have the same form, the individual Ni and Rh moment disturbances cannot be independently determined. We therefore define a new function as the sum of these two (spherically averaged) disturbances:

$$(1-c)G(K)+cH(K)\equiv\phi(K)=\sum_{R_i}Z_i\phi(R_i)\frac{\sin KR_i}{KR_i}\ . \tag{8}$$

Here, Z_i is the coordination number of the ith shell at distance R_i and $\phi(R_i)$ is the moment disturbance. We then assume that $\phi(R_i)$ beyond the nearest-neighbor shell decreases with a Yukawa dependence

$$\phi(R_i)=(R_1/R_i)\phi(R_1)e^{-\kappa(R_i-R_1)}\ , \tag{9}$$

and fit $M(K)/f_{Ni}$ with the parameters $(f_{Rh}/f_{Ni})\bar{\mu}_{Rh}-\bar{\mu}_{Ni}$, $\phi(R_1)$ and κ. The fitted functions are shown as the solid curves in Fig. 1 and the corresponding parameters are given in Table I. The curves describe the data quite well, thus indicating that the assumed form for $\phi(R_i)$ is reasonable. Furthermore, the fitted values of $M(0)$ agree with the magnetization values of $d\bar{\mu}/dc$ as shown by the arrows in Fig. 1 and by the last two columns of Table I. Local environment effects are therefore responsible for the moment fluctuations in Ni-Rh alloys.

These fluctuations are small and comparable to those caused by Cu in Ni. However, the range increases rapidly with increasing Rh content so that the total moment disturbance $M(0)$ of the concentrated alloys becomes much larger than for Ni-Cu. These parameters, of course, describe the weighted sum of the disturbances at the Ni and Rh

TABLE I. Moment disturbance parameters for Ni-Rh alloys.

at.% Rh	$(f_{Rh}/f_{Ni})\bar{\mu}_{Rh}-\bar{\mu}_{Ni}$	$\phi(R_1)$	κ	$M(0)$	$\frac{d\mu}{dc}$
10	−0.204	−0.020	0.41	−1.0	−0.85
15	−0.272	−0.049	0.73	−1.3	−1.4
25	−0.230	−0.042	0.34	−2.3	−2.3
30	−0.137	−0.036	0.26	−2.7	−2.7
35	−0.105	−0.018	0.14	−3.5	−3.4

TABLE II. Individual moment values for Ni-Rh alloys.

at.% Rh	$\bar{\mu}$[a]	$(f_{Rh}/f_{Ni})\bar{\mu}_{Rh}-\bar{\mu}_{Ni}$	$\bar{\mu}_{Rh}$	$\bar{\mu}_{Ni}$
2	0.644	±0.90	1.57 or −0.25±0.15	0.625 or 0.662
5	0.645	±0.56	1.20 or 0.12±0.10	0.616 or 0.673
10	0.615	−0.204	0.506±0.121	0.627
15	0.554	−0.272	0.375±0.080	0.586
25	0.371	−0.230	0.226±0.028	0.419
30	0.244	−0.137	0.167±0.024	0.277
35	0.116[b]	−0.105	0.053±0.013	0.150

[a] Magnetization data of Refs. 1 and 2 expressed in μ_B/atom.
[b] Average moment at 20 kOe.

sites and are not resolvable into the parameters for the individual Ni and Rh responses. Some insight into this resolution can be gained by determining the concentration dependence of the Ni and Rh moments and relating the concentration derivatives through Eqs. (5) and (6) to the net disturbance at each site.

The Ni and Rh moments are obtained by combining the $(f_{Rh}/f_{Ni})\mu_{Rh}-\bar{\mu}_{Ni}$ parameters with the bulk magnetization data. Results, given in Table II and Fig. 3, include the 2- and 5-at.% Rh data for which $[T(K)]^{1/2}=M(K)$ has been assumed. These exhibit little K dependence so we set $\phi(K)=0$ and obtain the moment difference parameters simply as a weighted average of the data shown in Fig. 2. At these two compositions, only unpolarized neutron data were obtained so only the magnitude and not the sign of these parameters are determined. This is indicated by the ± signs in Table II. The Rh and Ni moments for the positive (negative) solutions are given as the upper (lower) values in the table. The magnetization data show a positive $d\bar{\mu}/dc$ at 2-at.% Rh and this seems to go negative near 4- or 5-at.% Rh. With the present assumptions that $[T(0)]^{1/2}=M(0)=d\bar{\mu}/dc$, this would dicate the positive solution at 2-at.% Rh and the negative solution at 5-at.% Rh. However, since this results in a discontinuous concentration dependence for both the Rh and Ni moments and since $d\bar{\mu}/dc$ changes sign near 5-at.% Rh, we believe the positive solution at both compositions is more consistent with the combined data. These are the values shown in Fig. 3. The errors quoted in Table II for the Rh moments include counting statistics, fitting errors and uncertainties in the multiple Bragg scattering corrections. The errors for the Ni moments are essentially the same as for the magnetization data which are typically (1–2)%. Reference to Fig. 3 shows that the average Ni moment increases slightly to about 10-at.% Rh and then decreases while the average Rh moment is quite large at low c but decreases very rapidly with increasing Rh content.

It seems unlikely that this rapid decrease in the average Rh moment arises from antiferromagnetic Rh-Rh interactions since an antiparallel correlation of *aligned* Rh moments should appear as a peak in the $M(K)$ or $[T(K)]^{1/2}$ function near $K=1.5$ Å^{-1} where a dip is actually observed. A more likely mechanism is a strong local environment effect which destroys, or at least drastically reduces, the ferromagnetic Rh moment. Within this framework, it is interesting to compare the Rh moment behavior with the probability of nearest-neighbor configurations. One finds that the rapid decrease is best described by a P_{12} dependence where $P_{12}=(1-c)^{12}$ is the probability that an atom has 12 Ni nearest neighbors. This is il-

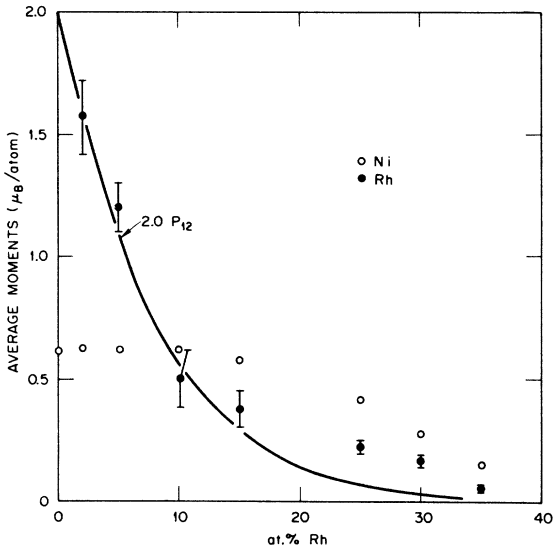

FIG. 3. Average moments at Rh and Ni sites vs concentration for Ni-Rh alloys. P_{12} is the probability that an atom has 12 Ni nearest neighbors.

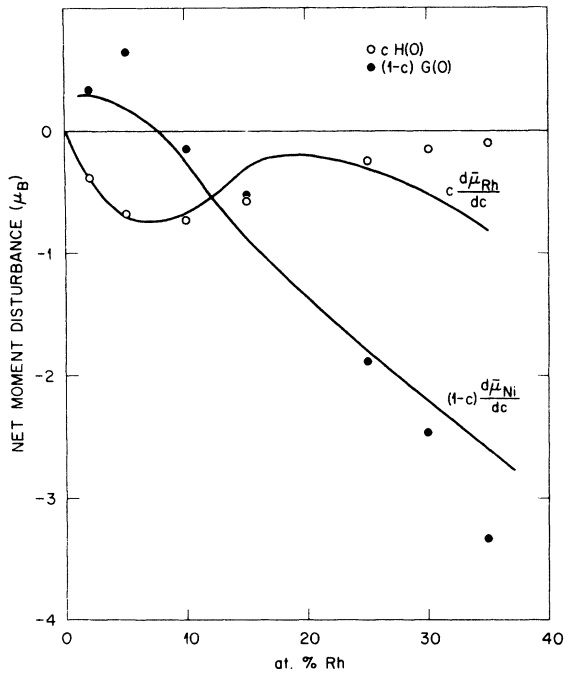

FIG. 4. Net moment distrubance at Ni and Rh sites. The solid curves are concentration derivatives taken from Fig. 3 and the points are calculated for the magnetic-environment model.

lustrated by the curve labelled $2P_{12}$ in Fig. 3 which passes through the inner data points and suggests a moment of $2\mu_B$ for isolated Rh atoms but a much smaller moment for those Rh atoms with one or more Rh nearest neighbors.

Having established the concentration dependence of the individual moments, we now take the concentration derivatives and use Eqs. (5) and (6) to obtain additional information regarding the moment disturbances at Ni and Rh sites. These derivatives, taken from smooth curves drawn through the data of Fig. 3 and weighted by the appropriate concentration factors, are shown as the solid curves in Fig. 4. The curves show that $cd\bar{\mu}_{\mathrm{Rh}}/dc$ is always small and negative while $(1-c)d\bar{\mu}_{\mathrm{Ni}}/dc$ starts positive, changes sign near 8-at.% Rh and attains large negative values at the higher Rh levels. From Eqs. (5), (6), and (8), we conclude that the disturbances at Ni and Rh sites tend to cancel in the dilute region but are both negative at 10-at.% Rh where the disturbance at Rh sites is the larger The disturbance at Ni sites dominates the cross section at the higher concentrations where the $\phi(R_1)$ and κ parameters in Table I can be regarded as approximately descriptive of the Rh-induced moment disturbances at Ni sites. As noted earlier, these increase in range with increasing Rh content. Since chemical-environment effects are largely due to short-range, charge-transfer effects, there is no apparent mechanism to explain the observed range increase on the basis of a purely chemical-environment model. However, if the moment on a Ni atom is assumed to depend on its magnetic environment, then any moment reduction at a Ni site is passed along sequentially to neighboring shells and there is a built-in mechanism for long-range moment disturbances. Such a model has been used[8] to explain the neutron data for the Ni-Cu system. The model not only provides a remarkable fit to the very precise Ni-Cu data, but also describes all available neutron diffuse scattering data for other nonmagnetic impurities in Ni with one parameter fixed by extrapolation of the Ni-Cu results and only one free parameter. In the next section, we extend this model to the Ni-Rh case.

IV. MAGNETIC-ENVIRONMENT MODEL

Although this model includes both chemical and magnetic-environment effects, we refer to it as the magnetic environment model for brevity. In this model, the moment on a Ni atom is assumed to be a function of the number of impurity nearest neighbors ν and of an effective exchange field H produced by its nearest neighbors. The moment on a Ni atom at site n is then

$$\mu_{\vec{n}}^{\mathrm{Ni}} = F(H_{\vec{n}}, \nu_{\vec{n}}), \tag{10}$$

where

$$H_{\vec{n}} = \sum_{\vec{\delta}} [J_{\mathrm{NiNi}}(1 - p_{\vec{n}+\vec{\delta}}) + J_{\mathrm{NiRh}}\, p_{\vec{n}+\vec{\delta}}]\mu_{\vec{n}+\vec{\delta}} \tag{11}$$

and

$$\nu_{\vec{n}} = \sum_{\vec{\delta}} p_{\vec{n}+\vec{\delta}}. \tag{12}$$

Here, the sums are over the $\vec{\delta}$ nearest neighbors and $p_{\vec{n}+\vec{\delta}}$ is a site occupation operator which is unity if there is a Rh atom at $\vec{n}+\vec{\delta}$ and is zero otherwise If the Ni moment fluctuations are small, we can expand about an effective field and $\langle\nu\rangle$, i.e.,

$$\mu_{\vec{n}}^{\mathrm{Ni}} = F(H_{\vec{n}}, \nu_{\vec{n}})$$

$$= F(H_{\mathrm{eff}}, \langle\nu\rangle) + \frac{\partial F}{\partial H}(H_{\vec{n}} - H_{\mathrm{eff}}) + \frac{\partial F}{\partial \nu}(\nu_{\vec{n}} - \langle\nu\rangle), \tag{13}$$

where

$$\bar{\mu}_{\mathrm{Ni}} = F(H_{\mathrm{eff}}, \langle\nu\rangle). \tag{14}$$

We now describe the Ni moment in terms of a fluctuation about the average as in the local-environment model of Sec. III:

$$\mu_{\vec{n}}^{Ni} = \bar{\mu}_{Ni} + \sum_{\vec{R}} g(\vec{R})(p_{\vec{n}+\vec{R}} - c). \quad (15)$$

The Rh moment is described as $2\mu_B$ for those Rh atoms surrounded by 12 Ni nearest neighbors and some smaller value μ_{Rh}^s otherwise, i.e.,

$$\mu_{\vec{n}}^{Rh} = (2 - \mu_{Rh}^s) \prod_{\vec{\delta}} (1 - p_{\vec{n}+\vec{\delta}}) + \mu_{Rh}^s, \quad (16)$$

where the product is for the $\vec{\delta}$ nearest neighbors of $\vec{n}$. Within the local environment model, the real-space moment disturbances are given by

$$g(\vec{R}) = \langle (p_{\vec{R}} - c)(1 - p_0)\mu_0 \rangle / c(1 - c)^2 \quad (17)$$

and

$$h(\vec{R}) = \langle (p_{\vec{R}} - c) p_0 \mu_0 \rangle / c^2(1 - c), \quad (18)$$

where $\vec{R} \neq 0$ and the angular brackets indicate configurational averages.

By substituting Eqs. (15) and (16) into Eq. (11) and Eq. (13) into Eq. (17), taking the configurational averages and Fourier transforming, one obtains

$$(1 - c)G(\vec{K}) = \{-\bar{\mu}_{Ni} + \rho Z_1 + \epsilon[\mu_{Rh}^s + (1 - c)^{10}(1 - 12c) \times (2 - \mu_{Rh}^s)]\} (\{B(\Gamma)[1 - \Gamma F_1(\vec{K})]\}^{-1} - 1). \quad (19)$$

Here, the following definitions have been used:

$$\Gamma = (1 - c) Z_1 J_{NiNi} \frac{\partial F}{\partial H}, \quad (20)$$

$$\rho\Gamma = (1 - c) \frac{\partial F}{\partial \nu}, \quad (21)$$

$$\epsilon = J_{NiRh}/J_{NiNi}, \quad (22)$$

$$F_1(\vec{K}) = \frac{1}{Z_1} \sum_{\vec{\delta}} e^{i\vec{K}\cdot\vec{\delta}}, \quad (23)$$

and

$$B(\Gamma) = \frac{1}{V} \int_{FBZ} d^3K \frac{1}{1 - \Gamma F_1(\vec{K})}, \quad (24)$$

where $B(\Gamma)$ is a known function of Γ.[8] We have also approximated the K dependence of the $(2 - \mu_{Rh}^s)$ term. This term arises from a correlation between nearest neighbors of nearest neighbors and extends to the fourth-neighbor shell in the fcc lattice. We take the $K = 0$ limit of this correlation $(1 - 12c)Z_1$ and assume a nearest-neighbor K dependence. This approximation is justified since the multiplying factor of $(1 - c)^{10}$ insures that this term is small for the concentrated alloys while the dilute alloys show very little K dependence.

The Rh moment disturbance is obtained by substituting Eq. (16) into Eq. (18), configurational averaging and Fourier transforming. The result is simply

$$cH(\vec{K}) = -c(1 - c)^{11}(2 - \mu_{Rh}^s) Z_1 F_1(\vec{K}). \quad (25)$$

Finally, the observed $M(K)$ is given by the spherical average of Eq. (3).

In fitting this model to the observed $M(K)$, we first note that μ_{Rh}^s is determined from $\bar{\mu}_{Rh}$ since the average of Eq. (16) is simply

$$\bar{\mu}_{Rh} = 2P_{12} + (1 - P_{12})\mu_{Rh}^s. \quad (26)$$

The Ni moment disturbance can then be written in terms of known values and functions as

$$(1 - c)G(K) = M(K)/f_{Ni} - \bar{\mu}_{Rh} f_{Rh}/f_{Ni} + \bar{\mu}_{Ni} - cH(K) f_{Rh}/f_{Ni}. \quad (27)$$

We then take the $K = 0$ limit of $G(K)$ and rewrite Eq. (19) as

$$(1 - c)G(K) = (1 - c)G(0)\left(\frac{B(\Gamma)(1 - \Gamma)}{1 - B(\Gamma)(1 - \Gamma)}\right) \times \left(\frac{1}{B(\Gamma)[1 - \Gamma F_1(K)]} - 1\right), \quad (28)$$

and fit Eq. (27) (known values) for the 15-, 25-, 30-, and 35-at.% Rh to Eq. (28) with the single parameter Γ. These Γ values are then used in the $K = 0$ limit of Eq. (19) to obtain values for

$$\{\rho Z_1 + \epsilon[\mu_{Rh}^s + (1 - c)^{10}(1 - 12c)(2 - \mu_{Rh}^s)]\}.$$

In this concentration range, μ_{Rh}^s is small and positive while the second term inside the curly brackets is small and negative. As a consequence, the ϵ term is unimportant and values of ρ are ob-

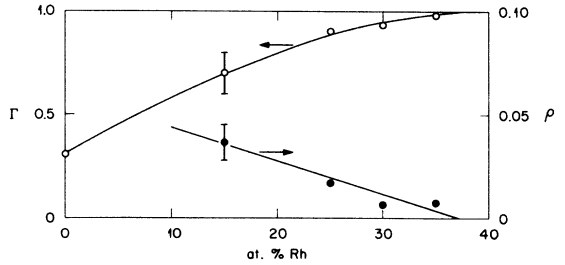

FIG. 5. Concentration dependence of the parameters Γ and ρ obtained by fitting the magnetic environment model to $M(K)$ for the four highest Rh content alloys. The point at $c = 0$ is an extrapolation of the Ni-Cu results from Ref. 8. The solid curves are intended only as a guide and have no theoretical basis.

tained directly. The resulting $M(K)$ curves for these four compositions are indistinguishable from those shown in Fig. 1 which were fitted to Eq. (8). The Γ and ρ parameters are shown in Fig. 5 and their concentration dependences are seen to approach the appropriate limits of one and zero, respectively, at the critical composition of 37-at.% Rh. Furthermore, the Γ values extrapolate reasonably to the value for pure Ni ($\Gamma_0 = 0.305$) previously obtained by extrapolation of the Ni-Cu results[8] and shown as the $c = 0$ point in Fig. 5. For the three more dilute alloys we take interpolated Γ values from Fig. 5 and find that the $(1-c)G(K)$ and $cH(K)$ functions almost cancel for the 2- and 5-at.% alloys while the $(1-c)G(K)$ term is negligible for the 10-at.% alloy. The corresponding $M(K)$ curves are compared with the data in Figs. 1 and 2 (dashed curves). The curves represent the 2- and 5-at.% data adequately but the 10-at.% data show a sharper K dependence than that given by the model. Agreement with the latter could, however, be improved by decreasing $M(0)$. Finally, a linear extrapolation of ρ into the dilute region allows a determination of ϵ. This parameter makes its most significant contribution at 2-at.% Rh where an extrapolated ρ value of 0.05 ± 0.02 yields $\epsilon = 0.6 \pm 0.2$.

This magnetic environment model gives an adequate representation of the data with reasonable parameters. The model is undoubtedly oversimplified since it neglects fluctuations in the small Rh moment. Some insight into the seriousness of this omission can be obtained by comparison of the $K = 0$ limits of the model with the appropriate concentration derivatives as shown in Fig. 4. The open data points are the $K = 0$ limits of Eq. (25), i.e., $cH(0) = -P_{11}(2 - \mu^s_{\mathrm{Rh}})$. These follow the observed $cd\overline{\mu}_{\mathrm{Rh}}/dc$ reasonably well out to 25-at.% Rh beyond which a divergence is found. The solid points are the $K = 0$ limits of Eq. (27), i.e.,

$$(1-c)G(0) = M(0) - \overline{\mu}_{\mathrm{Rh}} + \overline{\mu}_{\mathrm{Ni}} - cH(0).$$

These follow the general trend of $(1-c)d\overline{\mu}_{\mathrm{Ni}}/dc$ but seem to overestimate the Ni moment disturbance at 5-at.% Rh and in the region above 25-at.% Rh. The discrepancy at 5-at.% Rh probably just illustrates the difficulty in taking concentration derivatives, but the divergence in the high Rh content region is real and indicates that there are Rh moment fluctuations not included in the model. This dual divergence shows that the neglected Rh moment fluctuations have been treated as though they were Ni moment fluctuations. In the worst possible case (35-at.% Rh), however, this results in only a 27% overestimate of the latter. It seems then that the simple model in which the small Rh moment fluctuations are neglected is valid to 25-at.% Rh and still approximately valid even to 35-at.% Rh. It is possible to improve the model by inclusion of the Rh moment fluctuations but, in so doing, two additional parameters are introduced. It is doubtful that additional physical insight into the problem could be gained by fitting to the more complete model.

V. SUMMARY AND CONCLUSIONS

This study of the magnetic moment distribution in Ni-Rh alloys reveals several interesting effects. The $\overline{\mu}_{\mathrm{Rh}}$-vs-$c$ behavior strongly suggests moments of $2\mu_B$ for those Rh atoms surrounded by 12 Ni nearest neighbors and much smaller moments ($\sim 0.1\mu_B$) for other local chemical environments. This behavior correlates strongly with recent isolated cluster calculations[14] of the local susceptibilities for these alloys. Although restricted to the paramagnetic region, these calculations show that the local Rh susceptibility is strongly dependent on local chemical environment and diverges for 11 or 12 Ni nearest neighbors.

The agreement between $M(0)$ and $d\overline{\mu}/dc$ shows that the magnetic moment fluctuations are due to local environment effects. The range of these effects increases with increasing Rh content indicating that the magnetic environment is an important factor in the moment distribution of these alloys. The $M(K)$ data are fitted to an extended version of a previously described magnetic-environment model with physically reasonable parameters. The magnetic parameter Γ which appears in $G(K)$ as an exchange enhancement factor that determines the K dependence, is found to approach the correct limits at both extremes of the ferromagnetic region. This parameter approaches unity at the critical composition which is lower here (37-at.% Rh) than for Ni-Cu alloys (56-at.% Cu). This approach to unity depends on the shape of the response function $F(H, \nu)$ and this, in turn depends on the details of the d-band structure for the *ferromagnetic* alloys. Such calculations are not yet available for comparison with the present results.

The chemical parameter ρ appears in the cross section as part of the $K = 0$ limit of $G(K)$. The correct value for ρ is not known as $c \to 0$ but this parameter does approach the correct limit of zero at 37-at.% Rh. In contrast to the chemical effects for nonmagnetic impurities in Ni, which are all negative,[8] ρ is positive for Ni-Rh alloys. Thus, in the absence of magnetic effects, a Ni atom would have its moment increased by Rh nearest neighbors. This moment increase is given by $\partial F/\partial \nu = \rho\Gamma/(1-c)$ and amounts to only about $+0.02\mu_B$/Rh at the Ni rich end and $+0.01\mu_B$/Rh

in the critical region. From the concentration dependence of $\overline{\mu}_{Rh}$ and $\overline{\mu}_{Ni}$, both the magnetic and chemical effects tend to increase the Ni moments in the dilute region while the magnetic effect goes negative and becomes dominant for the more concentrated alloys.

ACKNOWLEDGMENTS

The author expresses his appreciation to R. A. Medina for numerous detailed discussions about this problem and to J. L. Sellers for technical assistance in the experiment.

*Research sponsored by the U. S. Energy Research and Development Administration under contract with Union Carbide Corp.

[1]J. Crangle and D. Parsons, Proc. R. Soc. A 255, 509 (1960).
[2]W. C. Muellner and J. S. Kouvel, Phys. Rev. B 11, 4552 (1975).
[3]J. B. Comly, T. M. Holden, and G. G. Low, J. Phys. C 1, 458 (1968).
[4]J. S. Kouvel and J. B. Comly, Phys. Rev. Lett. 24, 598 (1970).
[5]T. J. Hicks, B. Rainford, J. S. Kouvel, G. G. Low, and J. B. Comly, Phys. Rev. Lett. 22, 531 (1969).
[6]J. W. Garland and A. Gonis, in *Magnetism in Alloys*, edited by P. A. Beck and J. T. Waber (AIME, New York, 1972), p. 79.
[7]A. T. Aldred, B. D. Rainford, T. J. Hicks, and J. S. Kouvel, Phys. Rev. B 7, 218 (1973).
[8]R. A. Medina and J. W. Cable, Phys. Rev. B 15, 1539 (1977).
[9]J. W. Cable, E. O. Wollan, and H. R. Child, Phys. Rev. Lett. 22, 1256 (1969).
[10]J. W. Cable and R. A. Medina, Phys. Rev. B 13, 4868 (1976).
[11]W. Marshall, J. Phys. C 1, 88 (1968).
[12]E. Balcar and W. Marshall, J. Phys. C 1, 966 (1968).
[13]H. Luo and P. Duwez, J. Less-Common Metals 6, 248 (1964).
[14]J. van der Rest, F. Gautier, and R. Brouers, J. Phys. F 5, 995 (1975).